Journal of Experimental Botany, Vol. 67, No. 5 pp. 1545–1555, 2016
doi:10.1093/jxb/erv547 Advance Access publication 25 December 2015

RESEARCH PAPER

The *SHORT-ROOT*-like gene *PtSHR2B* is involved in *Populus* phellogen activity

Andreia Miguel[1,2], Ana Milhinhos[1,2,*], Ondřej Novák[3], Brian Jones[4,5] and Célia M. Miguel[1,2,†]

[1] Instituto de Biologia Experimental e Tecnológica (iBET), Apartado 12, 2781-901 Oeiras, Portugal
[2] Instituto de Tecnologia Química e Biológica António Xavier, Universidade Nova de Lisboa (ITQB-UNL), Avenida da República, 2780-157 Oeiras, Portugal
[3] Laboratory of Growth Regulators, Centre of the Region Haná for Biotechnological and Agricultural Research, Faculty of Science, Palacký University & Institute of Experimental Botany AS CR, Šlechtitelů 27, 783 71, Olomouc, Czech Republic.
[4] Umeå Plant Science Centre, Department of Plant Physiology, Umeå University, Umeå, Sweden
[5] Faculty of Agriculture, Food and Natural Resources, University of Sydney, Sydney, Australia

* Present address: Department of Plant Sciences, University of Oxford, Oxford OX1 3RB, UK.
† Correspondence: cmiguel@itqb.unl.pt

Received 14 September 2015; Accepted 2 December 2015

Editor: Bruno Moulia, UMR 547 PIAF Integrative Physics and Physiology of Trees

Abstract

SHORT-ROOT (SHR) is a GRAS transcription factor first characterized for its role in the specification of the stem cell niche and radial patterning in *Arabidopsis thaliana* (*At*) roots. Three *SHR*-like genes have been identified in *Populus trichocarpa* (*Pt*). *PtSHR1* shares high similarity with *AtSHR* over the entire length of the coding sequence. The two other *Populus SHR*-like genes, *PtSHR2A* and *PtSHR2B*, are shorter in their 5' ends when compared with *AtSHR*. Unlike *PtSHR1*, that is expressed throughout the cambial zone of greenhouse-grown *Populus* trees, *PtSHR2Bprom:uidA* expression was detected in the phellogen. Additionally, *PtSHR1* and *PtSHR2B* expression patterns markedly differ in the shoot apex and roots of *in vitro* plants. Transgenic hybrid aspen expressing *PtSHR2B* under the 35S constitutive promoter showed overall reduced tree growth while the proportion of bark increased relative to the wood. Reverse transcription–quantitative PCR (RT–qPCR) revealed increased transcript levels of cytokinin metabolism and response-related genes in the transgenic plants consistent with an increase of total cytokinin levels. This was confirmed by cytokinin quantification by LC-MS/MS. Our results indicate that *PtSHR2B* appears to function in the phellogen and therefore in the regulation of phellem and periderm formation, possibly acting through modulation of cytokinin homeostasis. Furthermore, this work points to a functional diversification of *SHR* after the divergence of the *Populus* and *Arabidopsis* lineages. This finding may contribute to selection and breeding strategies of cork oak in which, unlike *Populus*, the phellogen is active throughout the entire tree lifespan, being at the basis of a highly profitable cork industry.

Key words: Cytokinin, lateral meristem, phellogen, *Populus tremula*×*Populus tremuloides*, secondary growth, *SHORT-ROOT*.

Introduction

Plant growth occurs from specialized regions called meristems. Mitotic divisions in the meristems produce the cells that eventually differentiate into the organs and tissues that comprise the body of the plant. Four main meristems exist in woody perennials, the root and shoot apical meristems, that provide cells for shoot and root growth, respectively, and the

vascular cambium and cork cambium (phellogen) that generate cells for the secondary, or radial, growth of the stem, branches, and roots.

During secondary growth, the epidermis is replaced in the stems and roots by the periderm. This protective tissue is derived from the activity of the phellogen or cork cambium that forms a continuous ring of meristematic cells around the stem and roots. Periclinal divisions of the phellogen initials give rise to cells that differentiate into phelloderm towards the inside of the stem and into phellem towards the outside (Evert, 2006), in a way similar to the differentiation of vascular tissues from the vascular cambium. In a few species, of which the cork oak is an extreme example, the activity of the phellogen contributes to a significant enlargement of the trunk, producing a thick layer of phellem or cork. In adult cork oak trees, cork is regularly stripped from the tree and used for several industrial applications due to its exceptional impermeability, insulation, density, high energy absorption, resilience, and elasticity properties (Silva *et al.*, 2005).

Several lines of evidence have indicated that although the structure of the meristems differs, there are commonalities in the molecular mechanisms underlying their function (Schrader *et al.*, 2004; Baucher *et al.*, 2007; Du and Groover, 2010). Examples of genes known to be involved in the regulation of different meristems include the Class III *HD-ZIP* (Emery *et al.*, 2003; Schrader *et al.*, 2004; Du *et al.*, 2011; Robischon *et al.*, 2011), the *Populus* Class I *KNOX* homeobox genes *ARBORKNOX1* and *ARBORKNOX2* (*ARK1* and *ARK2*) which are orthologues of *Arabidopsis SHOOTMERISTEMLESS* (*STM*) and *BREVIPEDICELLUS* (*BP*), respectively (Long *et al.*, 1996; Mele *et al.*, 2003; Groover *et al.*, 2006; Du *et al.*, 2009; Liebsch *et al.*, 2014), *SHORT-ROOT* (*SHR*) (Benfey *et al.*, 1993; Fukaki *et al.*, 1998; Helariutta *et al.*, 2000; Schrader *et al.*, 2004; Dhondt *et al.*, 2010; Wang *et al.*, 2011), and *Arabidopsis WUSCHEL* (*WUS*) (Mayer *et al.*, 1998; Brand *et al.*, 2000; Schoof *et al.*, 2000) and *WUSCHEL-RELATED HOMEOBOX 5* (*WOX5*) (Haecker *et al.*, 2004; Schrader *et al.*, 2004; Baucher *et al.*, 2007; Sarkar *et al.*, 2007; Tucker and Laux, 2007; Stahl and Simon, 2009; Stahl *et al.*, 2009). Although considerable attention has been paid to the functioning of the apical meristems and the vascular cambium, little is known about the functioning of the phellogen, despite its critical importance in establishing a protective layer on stems, branches, and roots. Given the existing evidence, it can be hypothesized that the mechanisms underlying phellogen function will overlap those of the other meristems (Soler, 2008).

The SHR transcription factor belongs to the GRAS family of plant-specific proteins that are characterized by a variable N-terminal domain but a highly conserved C-terminal domain (Helariutta *et al.*, 2000; Bolle, 2004). The *Arabidopsis* SHR (AtSHR) has been well characterized, being a key regulator, along with the related GRAS protein SCARECROW (SCR), of radial patterning and stem cell niche specification in the roots (Benfey *et al.*, 1993; Di Laurenzio *et al.*, 1996; Helariutta *et al.*, 2000; Nakajima *et al.*, 2001). It is essential for the asymmetric cell divisions of the cortex/endodermal initial (CEI) (Benfey *et al.*, 1993; Helariutta *et al.*, 2000; Nakajima *et al.*, 2001), and for the periclinal divisions of cortex cells in a maturing root (Paquette and Benfey, 2005). Fukaki *et al.* (1998) demonstrated that *AtSHR* is also involved in radial patterning in the shoot. More recently, Dhondt *et al.* (2010) demonstrated that, similarly to the *Arabidopsis* root, SHR functions in association with its downstream target, SCR, in the regulation of cell proliferation and vascular differentiation in leaves. The SHR/SCR mechanism therefore appears to have been co-opted to regulate cell proliferation and differentiation in multiple organs.

SHR modulates the expression of genes involved in a wide range of processes during *Arabidopsis* root development, including transcriptional regulation, signalling, and response to hormones, and in the regulation of cell cycle genes (Levesque *et al.*, 2006; Sozzani *et al.*, 2010). In *Arabidopsis*, correct patterning of the central vascular cylinder is mediated through movement of the SHR protein from the stele into the endodermis (Nakajima *et al.*, 2001), where it activates its target, SCR, that together activate *miR165a* and *miR166b* (Carlsbecker *et al.*, 2010). The regulation of vascular patterning by SHR in the *Arabidopsis* root involves the modulation of cytokinin (CK) homeostasis through the direct regulation of the cytokinin-degrading enzyme, *CYTOKININ OXIDASE 3* (*CKX3*) (Cui *et al.*, 2011; Hao and Cui, 2012).

SHR has also been studied in tree species such as *Pinus radiata*, where it was suggested to have roles in root meristem formation and maintenance, and in the cambial region of hypocotyls (Solé *et al.*, 2008). The putative *Populus* orthologue of *AtSHR*, *PtSHR1*, is expressed in the cambial zone (Schrader *et al.*, 2004; Wang *et al.*, 2011) and functions as a regulator of cell division and meristem activity in the shoots (Wang *et al.*, 2011). Partial suppression of the *PtSHR1* transcript in transgenic lines leads to taller trees with a larger vascular cambium due to an increase in cell proliferation in the cambial zone (Wang *et al.*, 2011). In both *Arabidopsis* and *Populus*, it has been suggested that *SHR* regulates growth through the control of cell divisions, in a concentration-dependent manner (Paquette and Benfey, 2005; Wang *et al.*, 2011; Koizumi *et al.*, 2012).

Whereas there is only one *SHR* gene in *Arabidopsis*, three *SHR*-like genes have been identified in the *Populus* genome, *PtSHR1*, *PtSHR2A*, and *PtSHR2B* (Wang *et al.*, 2011). Based on sequence similarity and on functional studies with the *PtSHR1* coding sequence, driven by the *AtSHR* promoter, *PtSHR1* is considered to be the putative ortholog of the *Arabidopsis SHR* (Wang *et al.*, 2011). In this study, *PtSHR2B* was investigated in order to better understand its role in meristem function in hybrid aspen. We show that *PtSHR2B* is expressed in the phellogen, pointing to a regulatory role in this meristem during secondary growth. Overexpression of *PtSHR2B* in hybrid aspen not only affected overall plant growth, but altered the ratio between the amount of wood and bark tissues in the stem. We further present experiments that indicate that *PtSHR2B* may act, at least partially, through the regulation of CK homeostasis.

Materials and methods

Plant material

Hybrid aspen (*Populus tremula* L.×*Populus tremuloides* Michx.; Clone T89) was propagated *in vitro* on half-strength basal MS medium (Murashige and Skoog, 1962) and maintained in a growth chamber at 21 °C in a 16 h light/8 h dark photoperiod. For greenhouse experiments, *in vitro* established wild-type and transgenic plants were placed in a soil:peat:perlite (1:3:1) potting mix and acclimatized in a growth chamber, gradually decreasing the humidity from 95% to 70% over 5 weeks before transfer to the greenhouse, where plants were grown for a minimum of 10 weeks prior to analysis. The position of all pots within the greenhouse was changed weekly to minimize positional bias experimental error.

After 10 weeks in the greenhouse, the five youngest fully expanded leaves were collected (Supplementary Fig. S1A at *JXB* online). Bark was isolated by peeling off the stem across the cambial zone. The remaining stem tissues (xylem and pith), hereafter termed 'wood', were collected together. All samples were immediately frozen in liquid nitrogen and stored at –80 °C until further processing. Intact stem sections were also collected and fixed in FAA (5% formaldehyde, 5% acetic acid, 50% ethanol) for anatomical analysis.

Gene constructs and genetic transformation

To detect promoter activity of *PtSHR1*, *PtSHR2A*, and *PtSHR2B*, transgenic lines were generated using constructs incorporating ~2.5 kbp sequence upstream of the start codon of each of the genes, fused to the coding sequence of *uidA* encoding β-glucuronidase (GUS) (*PtSHR*$_n$*prom:uidA*), using the pKGWFS7,0 binary vector (Karimi *et al.*, 2002). The sequences (eugene3.01860017, eugene3.00070144, and eugene3.00640143, for *PtSHR1*, *PtSHR2A*, and *PtSHR2B*, respectively) were retrieved from the *Populus trichocarpa* genome version v1.1 (http://genome.jgi-psf.org/Poptr1_1/Poptr1_1.home.html) and were previously described by Wang *et al.* (2011). In Phytozome v9.1 (http://www.phytozome.net/), the corresponding loci are Potri.007G063300, Potri.007G132000, and Potri.017G019900 for *PtSHR1*, *PtSHR2A*, and *PtSHR2B*, respectively. To express *PtSHR2B* ectopically, its coding sequence was cloned downstream of the 35S *Cauliflower mosaic virus* (CaMV) promoter in the pK7WG2,0 vector (*35S:PtSHR2B*) (Karimi *et al.*, 2002). Hybrid aspen stem sections were transformed according to Nilsson *et al.* (1992). Ten independent transgenic lines were generated for each construct. Representative *PtSHR1prom:uidA* and *PtSHR2Bprom:uidA* lines and three independent overexpression lines, 2B_7, 2B_8, and 2B_12, were chosen for further analysis, after checking for the presence of single insertion events by Southern blot analysis. In this study, the nomenclature and the gene sequence information followed Wang *et al.* (2011).

Histochemical GUS assay

GUS assays were performed in transformed hybrid aspen leaves, roots, and shoot apex collected from 6-week-old *in vitro* grown shoots, and 6-month-old and 1-year-old stems of greenhouse-grown trees. Tissues were placed in ice-cold 90% acetone for 30 min and then washed in water prior to immersion in the GUS staining solution [10 mM sodium phosphate buffer pH 7.0, 0.5% Triton X-100, 2 mM potassium ferricyanide, and 2 mM X-Gluc (5-bromo-4-chloro-3-indolyl β-D-glucuronide)], vacuum infiltrated, and incubated overnight in the dark at 37 °C. After washing in water, tested leaves, roots, and shoot apex of *in vitro* plants were gradually dehydrated to 70% ethanol and stem sections of the greenhouse-grown plants were fixed in FAA and then included in Technovit 7100 resin (Heraeus Kulzer), according to the manufacturer`s instructions, with minor modifications: after vacuum infiltration, samples were left for 2 d at 4 °C in the pre-infiltration solution. The solution was then replaced and samples left for another 7 d at 4 °C. The material was subsequently placed in the infiltration solution and left for 1–3 weeks at 4 °C, followed by polymerization at room temperature.

Stereomicroscope observations were performed with a Nikon SMZ800, and images were captured using an Olympus SC30 camera and software. Microscope observations were made with a Nikon Inverted Microscope Eclipse TE300, and images taken with a Nikon DS-Fi1 camera using the NIS-Elements F3.0 software.

Anatomical analysis and growth measurements

Stem pieces of 1- and 2-year-old shoots of wild-type hybrid aspen were collected and fixed in ice-cold FAA, as previously described, vacuum infiltrated, and left overnight in a desiccator at 4 °C. After gradual dehydration to 100% ethanol, tissues were embedded in resin as described above, and 6–8 µm thick sections were stained with Toluidine Blue O. Several growth parameters were analysed in 10-week-old greenhouse-grown *35S:PtSHR2B* trees (Supplementary Fig. S1A). Tree height and total length between the 10th (EN10) and the 17th (EN17) internodes from the shoot tip were recorded. Stem diameters were measured at the reference internode (EN14), showing fully differentiated secondary vascular tissues and chosen for comparison between transgenic and wild-type plants, and at the stem base (ENbase), corresponding to an internode between the 20th and 25th internodes depending on the tree. Measurements of distances between different stem tissues were taken at a minimum of four positions around the circumference of the stem sections using ImageJ software (Abràmoff *et al.*, 2004; Schneider *et al.*, 2012) (Supplementary Fig. S1B). The total lamina area of the five leaves surrounding EN14 was determined using a leaf area meter (LI-3000A, LI-COR Inc.).

Reverse transcription–quantitative PCR (RT–qPCR)

The first five fully expanded leaves down from the shoot tip, and bark and wood from the ENbase were collected and ground to a fine powder (Supplementary Fig. S1A) using either a mortar and pestle (leaves and bark) or a grinder mill (M 20 Universal mill, Ika). Isolation of bark and wood tissues was done as described in the 'Plant material' section. Total RNA from leaves and bark was isolated as described by Reid *et al.* (2006) with minor modifications (Marum *et al.*, 2012). Total RNA from wood samples was extracted using the protocol as described in Chang *et al.*, (1993), and all RNA samples were treated with TURBO DNase (Ambion) according to the manufacturer`s instructions. cDNA synthesis was performed from 1.5 µg of DNase-treated RNA, using a Transcriptor High Fidelity cDNA Synthesis Kit (Roche) with anchored oligo(dT)$_{18}$ primers. Quantitative real-time PCR (qPCR) was carried out in 96-well plates in a LightCycler 480 (Roche) using SYBR Green I Master Mix (Roche). Primers for amplifying a transcript fragment of *PtSHR2B*, 5'F-CAGCAATACCCTTTGCACACAG-3' and 5'R-ACCCAGTCCTTCCTTTGTG-3', were designed using the *P. trichocarpa* genome version 1.1 (http://genome.jgi-psf.org/Poptr1_1/Poptr1_1.home.html) and the gene sequence (eugene3.00640143) described by Wang *et al.* (2011). For amplification of *PtCKX3* (Potri.006G152500.1) transcripts, specific primers 5'F-TCAGATCCAAACCCTTGATTTC-3' and 5'R-CAGTAAAAGGGGTGTAGTT-3' were designed using *P. trichocarpa* genome version 3, from Phytozome (http://www.phytozome.net/). For amplification of *PtRR7* transcripts (Potri.016G038000.1), primers were as previously described (Nieminen *et al.*, 2008). *PtCYP2* (Potri.004G168800.1) was used as a reference gene (Brunner *et al.*, 2004; Milhinhos *et al.*, 2013). The PCR program used was 95 °C for 10 min, 45 cycles of 10 s at 95 °C, 20 s at 60 °C for *PtRR7* and *PtCKX3* or 20 s at 63 °C for *PtSHR2B*, and 10 s at 72 °C. The annealing temperature for the reference gene primers was 60 °C or 63 °C, depending on the experiment. Three technical replicates were used for each of the three biological samples in each experiment. To normalize values obtained from different plates, a calibrator sample consisting of cDNA synthesized

from RNA from leaves of a transgenic line was used in each plate. Normalized relative quantities were obtained through the $\Delta\Delta C_T$ method (Livak and Schmittgen, 2001; Pfaffl, 2001; Hellemans *et al.*, 2007) and the amplification efficiency determined using Real-Time PCR Miner (Zhao and Fernald, 2005).

Quantification of cytokinins

To quantify the CK levels in bark and wood tissues, samples were ground into a fine powder. CKs were extracted and isolated from ~10 mg of frozen tissues from bark and wood as previously described (Svačinová *et al.*, 2012), including modifications described by Antoniadi *et al.* (2015). To each extract, the stable isotope-labelled CK internal standards (0.1 pmol of CK bases, ribosides, *N*-glucosides, 0.25 pmol of *O*-glucosides, and 0.5 pmol of nucleotides) were further added as a reference. Purified samples were analysed by an LC-MS/MS system consisting of an ACQUITY UPLC® System (Waters) and a Xevo™ TQ-S (Waters) triple quadrupole mass spectrometer. Quantification was obtained using a multiple reaction monitoring (MRM) mode of selected precursor ions and the appropriate product ion. Five independent biological replicates were analysed for each sample.

Statistical analysis

The assessment of statistical significance in transcript profiles and phenotypic parameters was carried out using non-parametric analysis, Mann–Whitney U-test. A significance level of P=0.05 was used. An ANOVA was performed to assess the statistical significance in the quantification of CKs. Statistics were performed using the Statistica (StatSoft Inc., http://www.statsoft.com) software package.

Results

In this work, the *Populus SHR*-like gene *PtSHR2B* was characterized and compared with the putative *Populus* orthologue of the *Arabidopsis SHR* gene, *PtSHR1* (Wang *et al.*, 2011). *AtSHR* and *PtSHR1* genes have been previously implicated in the regulation of primary apical meristems and vascular cambium activity. Transverse sections of hybrid aspen stems at different developmental stages showed a distinct phellogen meristematic layer, already present at the end of the first year of growth and characterized by rectangular cells that are flattened radially and divide mostly by periclinal division (Supplementary Fig. S1C). The characteristic layer of suberized phellem cells in the periderm could be observed. The periderm in 2-year-old stems had only a slight increase in phellem layer thickness compared with 1-year-old stems (Supplementary Fig. S1C, D).

PtSHR1 and PtSHR2B show different expression patterns

While tissues from wild-type controls were always negative to GUS histochemical assay (Fig. 1A–D), analysis of hybrid aspen plants carrying either the *PtSHR1* or *PtSHR2B* promoter driving *uidA* expression (*PtSHR$_n$prom:uidA*) indicated different patterns of promoter activity. Analysis of *PtSHR1* promoter activity in greenhouse-grown trees that had undergone substantial secondary growth showed GUS throughout the cambial zone and in xylem rays (Fig. 1E, F). Additionally, *GUS* expression was found in the leaf vasculature and in the root stele of *in vitro* plants (Fig. 1G, H), similarly to its homologue in *Arabidopsis* (*AtSHR*) (Helariutta *et al.*, 2000; Dhondt *et al.*, 2010; Wang *et al.*, 2011). In the shoot apex, GUS staining was observed in the apical meristem and vasculature (Fig. 1I). In the case of the *PtSHR2B* promoter, the greenhouse-grown trees showed GUS staining strongly localized in the phellogen cell layer (Fig. 1J, K), suggesting a specific function for the modified version of SHR in this meristem. In leaves from *in vitro* plants, *GUS* expression was not detected (Fig. 1L), but in the roots GUS staining showed a stark contrast to that observed with the *PtSHR1* promoter, with *GUS* expression being observed at the root tip (Fig. 1M). Differences between the expression driven by each of the two promoters were also found in *in vitro* developing shoot tip where *PtSHR2Bprom:uidA* staining was restricted to apical and axillary meristems (Fig. 1N). Since no GUS signal was ever detected in any of the analysed tissues from plants carrying the *PtSHR2Aprom:uidA* construct, the study only proceeded with the analysis of *PtSHR2B*.

Profiling of *PtSHR2B* transcript levels by RT–qPCR in the tissues of wild-type greenhouse-grown hybrid aspen revealed the highest levels in the bark, with significantly lower levels in wood and leaf tissues (Fig. 2). These results corroborate the GUS staining observations, confirming that expression is predominantly in the phellogen, although not restricted to it (Figs 1J, K, 2).

Ectopic expression of PtSHR2B reduces overall tree growth

To explore the role of *PtSHR2B* in hybrid aspen, the *PtSHR2B* coding region was isolated and transformed into hybrid aspen under the control of the constitutive CaMV 35S promoter. RT–qPCR confirmed the ectopic expression of *PtSHR2B* in leaves and stem tissues of *in vitro 35S:PtSHR2B* plants (Fig. 3A). However, in the greenhouse-grown trees, the increased accumulation of *PtSHR2B* transcript was observed in leaves and bark, but not in wood tissues (Fig. 3B). No obvious phenotype could be observed in *in vitro* grown plants. However, 10-week old greenhouse-grown transgenic trees showed a reduced growth compared with the wild type (Fig. 4; Supplementary Fig. S2). Tree height in all of the transgenic lines was significantly reduced when compared with the wild-type plants (Fig. 4A, B). Both control and transgenic trees experienced growth deceleration between weeks 7 and 10, possibly due to a greenhouse temperature increase during this period. Stem diameter was significantly reduced compared with the wild type at the base of the transgenic trees (Fig. 4C) although no change could be observed in the reference internode (EN14). The reduction in height in the transgenic trees was primarily the result of a reduced internode length, as the mean internode length between EN10 and EN17 was significantly shorter in the transgenic trees compared with the wild type (Fig. 4D). The total number of internodes was slightly reduced, but this was only significant in one of the transgenic lines (Fig. 4E). The

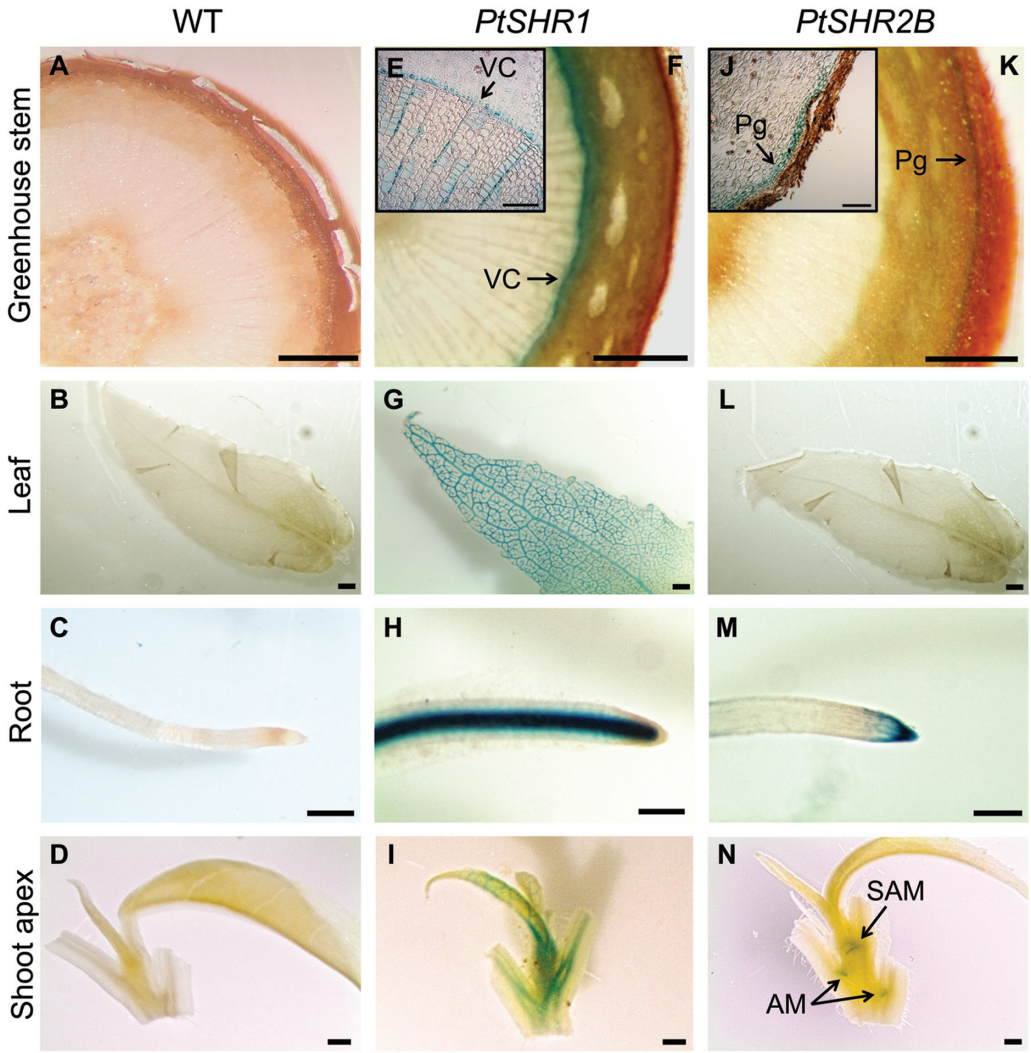

Fig. 1. Localization of *PtSHR1* and *PtSHR2B* promoter-driven *uidA* expression. (A, C–E, F, I–K, L–N, Q–S) GUS histochemical assay in 6-week-old hybrid aspen *in vitro* grown plants. (B, G, H, O, P) GUS histochemical assay in stems from 6-month-old greenhouse-grown hybrid aspen. Images A, F, G, L–N and O were taken under the microscope (scale bars=100 μm). Images B–E, H–K, and P–S were taken under the stereomicroscope (scale bars=475 μm). AX, axillary meristems; Pg, phellogen; SAM, shoot apical meristem; VC, vascular cambium.

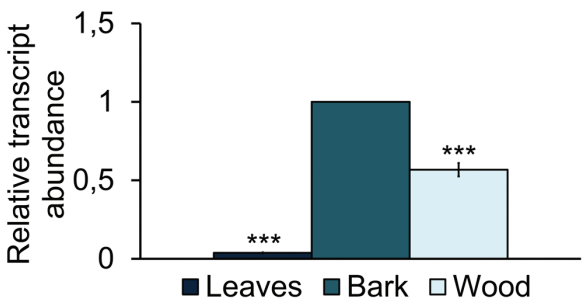

Fig. 2. Relative expression levels of *PtSHR2B* in tissues of wild-type hybrid aspen grown in the greenhouse for 10 weeks. Results are expressed relative to the expression in the bark, and values are the means ±SE of at least four biological replicates, except for wood where a mix of different wild-type plants was used, and three technical replicates. Asterisks indicate the significance of the difference between each tissue and the bark. (This figure is available in colour at *JXB* online.)

total average fresh weight and lamina area of the five leaves surrounding the reference internode was also significantly reduced in the transgenic trees (Fig. 4F, G).

Altered stem anatomy in 35S:PtSHR2B ectopic expression plants

Transverse sections taken from stems of the *35S:PtSHR2B* transgenic trees were analysed by light microscopy. The secondary xylem [radial distance from the pith side of the lignified xylem to the cambial zone (Supplementary Fig. S1B)] was significantly reduced in the transgenic trees compared with the wild type in two of the three transgenic lines (Fig. 5A), whereas the bark layer was wider than in the wild type (Fig. 5A). The difference in the proportion of wood and bark tissues was more evident at the base of the stem, where secondary growth is far more extensive (Fig. 5B). Additionally, the ratio between the phellem and the stem radius was reduced in two out of the three transgenic lines (Fig. 5C, D). Some variation was seen between the independent transformant lines, which is commonly observed and consistent with previous work using *Populus* (Robischon *et al.*, 2011; Milhinhos *et al.*, 2013).

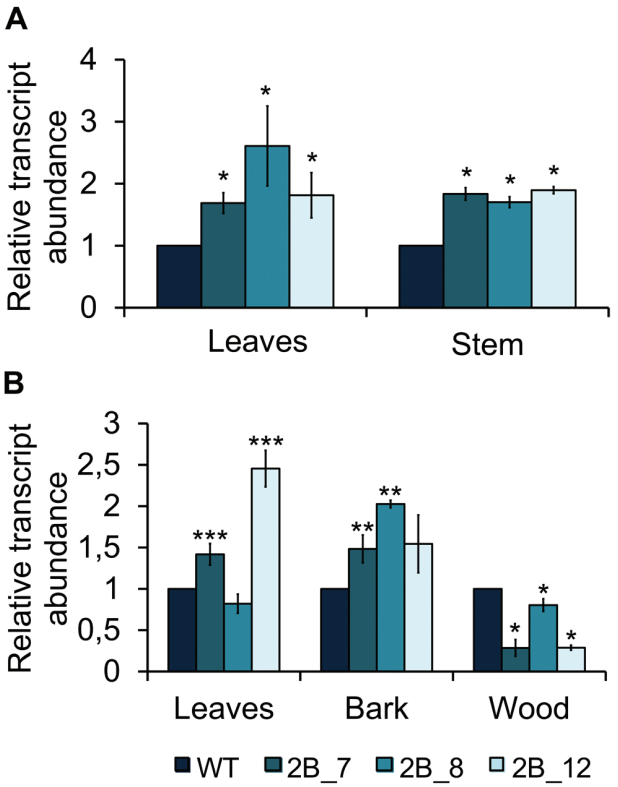

Fig. 3. Relative expression levels of *PtSHR2B* in tissues of hybrid aspen. (A) *PtSHR2B* transcript levels in 4-week-old *in vitro* grown *35S:PtSHR2B* plants. Values are the means ±SE of three biological and three technical replicates. (B) *PtSHR2B* transcript levels in *35S:PtSHR2B* trees grown in a greenhouse for 10 weeks. Values are the means ±SE of at least two biological and two technical replicates. Asterisks indicate the significance of the difference between each individual line and the wild type (*$P<0.05$, **$P<0.01$, and ***$P<0.001$, Mann–Whitney U-test). (This figure is available in colour at *JXB* online.)

Genes involved in cytokinin metabolism and response are altered in transgenic plants

CK has been linked to SHR function in *Arabidopsis* roots where SHR controls vascular patterning through its effect on CK homeostasis (Cui *et al.*, 2011). We analysed the transcript levels of a central CK primary response gene, the A-type response regulator *PtRR7* (Nieminen *et al.*, 2008; Ramírez-Carvajal *et al.*, 2008), in bark and wood tissues of the *35S:PtSHR2B* transgenic trees. *PtRR7* transcript levels were higher in the bark of all *PtSHR2B* overexpression lines compared with the wild type (Fig. 6A), indicating altered CK signalling in this tissue.

In *Arabidopsis* roots, SHR is known to act, at least partially, by directly regulating the expression of *CYTOKININ OXIDASE 3*, *AtCKX3* (Cui *et al.*, 2011). We also analysed transcript levels for the putative *Populus AtCKX3* orthologue, *PtCKX3*, in bark and wood tissues of the transgenic plants. Transcripts for *PtCKX3* were more abundant in the bark of the transgenic trees, compared with the wild type (Fig. 6B). Increased transcript levels for these genes in the bark indicate that *PtSHR2B* levels are important for the regulation of CK metabolism in this tissue. Transcript levels for both genes were also increased in wood tissue (Fig. 6A, B), but to a lesser extent than in bark and only in some transgenic lines.

Quantification of cytokinins in stem tissues

To clarify the link between *PtSHR2B* and CK homeostasis, we quantified the levels of CKs present in wood and bark tissues of the transgenic trees. Naturally occurring CKs are adenine derivatives with either isoprenoid or aromatic side chains. Isoprenoid CKs can be distinguished as isopentenyladenine (iP)-, *trans*-zeatin (tZ)-, *cis*-zeatin (cZ)-, or dihydrozeatin (DHZ)-type derivatives, depending on the hydroxylation and reduction of the side chain (Ha *et al.*, 2012). Total CK levels were altered in both tissues, as was the distribution of its derivatives (Fig. 7; Table 1). All *35S:PtSHR2B* transgenic trees presented high levels of total CKs in bark but lower levels in wood tissues (Fig. 7).

Discussion

The vascular cambium functioning and the development of vascular tissues have been the subject of numerous reports (Baucher *et al.*, 2007; Du and Groover, 2010; Schuetz *et al.*, 2012; Sanchez *et al.*, 2012). In contrast, despite the important role that the phellogen plays in providing cells for the development of the protective layer on stems, branches, and roots, it has received minimal attention. Under our growth conditions, a surrounding meristematic phellogen and a phellem (cork) layer had formed in 1-year-old hybrid aspen stems. The thickness of this layer was almost unchanged between 1- and 2-year-old hybrid aspen stems. Consistency in the phellem layer thickness during the lifespan of the close relative *Populus tremuloides* Michx. has long been known (Kaufert, 1937), indicating that in *Populus* species phellogen cell divisions are matched by a shedding of cork layer cells.

Populus is recognized as a model species in the study of angiosperm tree function. It has a high annual rate of secondary growth, and like other model species has the advantages of being relatively easily genetically modified and cultured. There are also now ample molecular, genomic, and bioinformatics resources available for various *Populus* species. Importantly, the *P. trichocarpa* genome has been fully sequenced (Tuskan *et al.*, 2006). The sequence data indicate that two whole-genome duplication events occurred in ancestors of the species (Tuskan *et al.*, 2006). Although duplicated genes are often lost over evolutionary time, higher gene retention is often found, particularly for specific classes of genes, such as: (i) genes with regulatory functions, namely transcription factors and developmental regulators (Blanc and Wolfe, 2004; Seoighe and Gehring, 2004; Carretero-Paulet and Fares, 2012); and (ii) for genes derived from a previous round of genome duplication (Seoighe and Gehring, 2004). The biased retention is most probably because multiple copies of the retained genes impart specific beneficial effects for the organism (Seoighe and Gehring, 2004; Carretero-Paulet and Fares, 2012). One of the ways in which multiple genes can be beneficial is through speciation, leading to divergent function and expression patterns (Blanc and Wolfe, 2004; Tuskan *et al.*, 2006; Rodgers-Melnick *et al.*, 2012). In *Populus*, it has been hypothesized that after duplication, gene preservation is influenced by a combination of subfunctionalization and

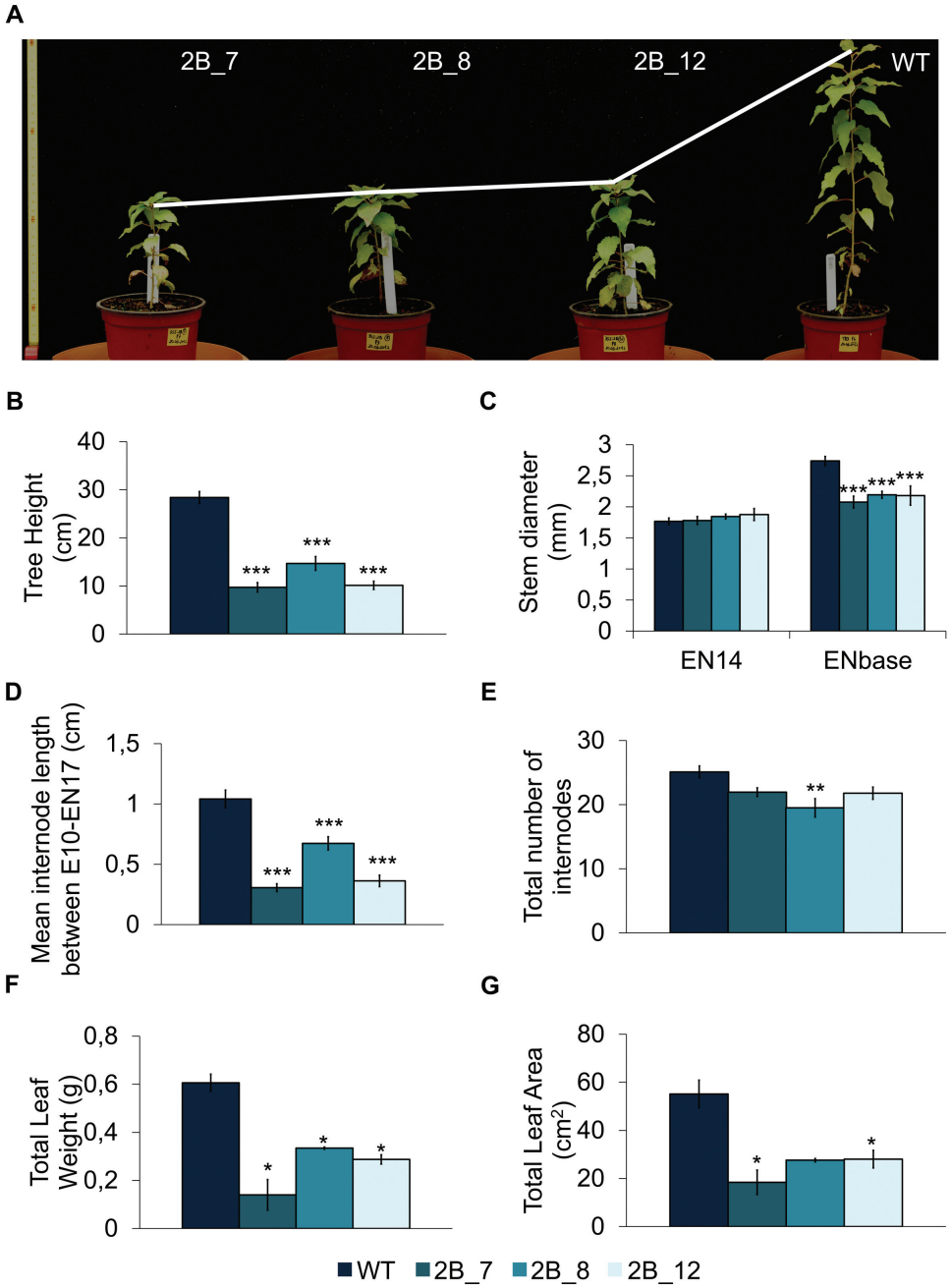

Fig. 4. Phenotypic characterization of transgenic *35S:PtSHR2B* hybrid aspen lines grown in the greenhouse for 10 weeks. (A) The wild type (WT) and plants from independent transgenic lines (2B_7; 2B_8 and 2B_12). (B) Tree height. Values are the means ±SE of at least eight biological replicates. (C) Stem diameter at the reference internode (EN14) and at the stem base (ENbase) corresponding to the 20th–25th internode. Values are the means ±SE of at least six biological replicates. (D) Mean internode length between the 10th and the 17th internodes (EN10 and EN17). Values are the means ±SE of at least eight biological replicates. (E) Total number of internodes. Values are the means ±SE of at least eight biological replicates. (F) Total weight of the five leaves surrounding EN14. Values are the means ±SE of at least thee biological replicates. (G) Total area of the leaves surrounding EN14. Values are the means ±SE of at least three biological replicates. Asterisks indicate the significance level between each individual line and the WT (**P*<0.05, ***P*<0.01, and ****P*<0.001, Mann–Whitney U-test). (This figure is available in colour at *JXB* online.)

selection favouring retention of genes that encode proteins with a large number of interactions (Rodgers-Melnick *et al.*, 2012). The presence of three *SHR*-like genes in the *Populus* genome indicates that *SHR* fits these criteria. In this work we show that the patterns of *GUS* expression driven by *Populus PtSHR1* and *PtSHR2B* promoters differ markedly both in the shoot apex and in the roots. Commensurate with *AtSHR* expression in *Arabidopsis*, GUS staining in the roots of the *PtSHR1prom:uidA* plants was confined to the stele. In contrast, the *PtSHR2B* promoter activity was detected in the root tip, suggesting that the two genes have different functions in the root. In greenhouse-grown plants with extensive secondary growth, *GUS* expression driven by both *PtSHR1* and *PtSHR2B* promoters was strongly associated with the lateral meristems. However, while GUS staining was detected in the vascular cambium of the *PtSHR1prom:uidA* plants, the

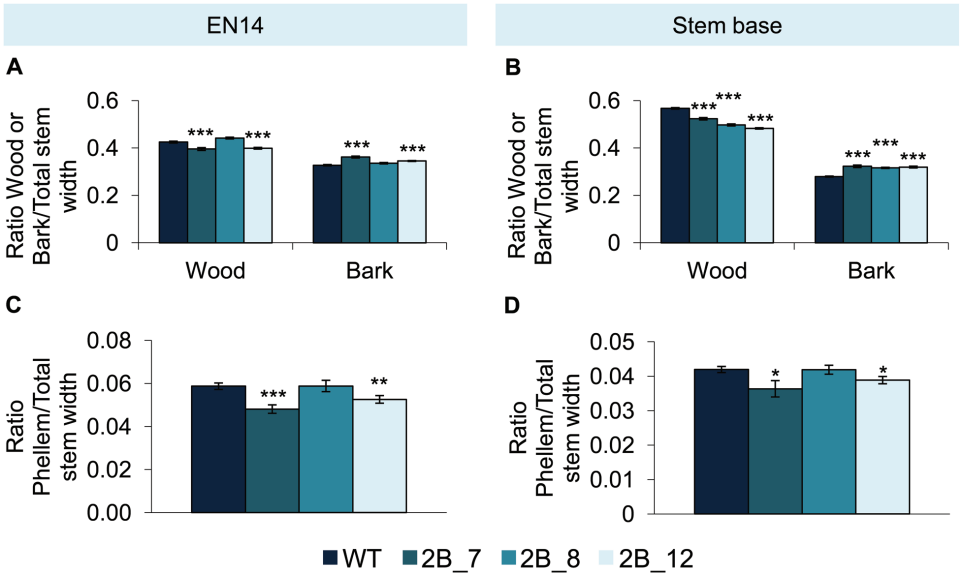

Fig. 5. Anatomical characterization of the *35S:PtSHR2B* hybrid aspen stems at the 14th internode (EN14) and at the stem base (ENbase) corresponding to an internode between the 20th and 25th internodes. (A and B) Ratio between the width of the wood or the bark layer and the stem radius at EN14 (A) and ENbase (B). (C and D) Ratio between the width of the phellem layer and the stem radius at EN14 (C) and ENbase (D). Values are the means ±SE of at least three biological replicates, and asterisks indicate the significance of the difference between each individual line and the wild type (**P*<0.05, ***P*<0.01, and ****P*<0.001, Mann–Whitney U-test). For each tree cross-section, the measurements were taken at a minimum of four equidistant positions around the circumference of the stem. (This figure is available in colour at *JXB* online.)

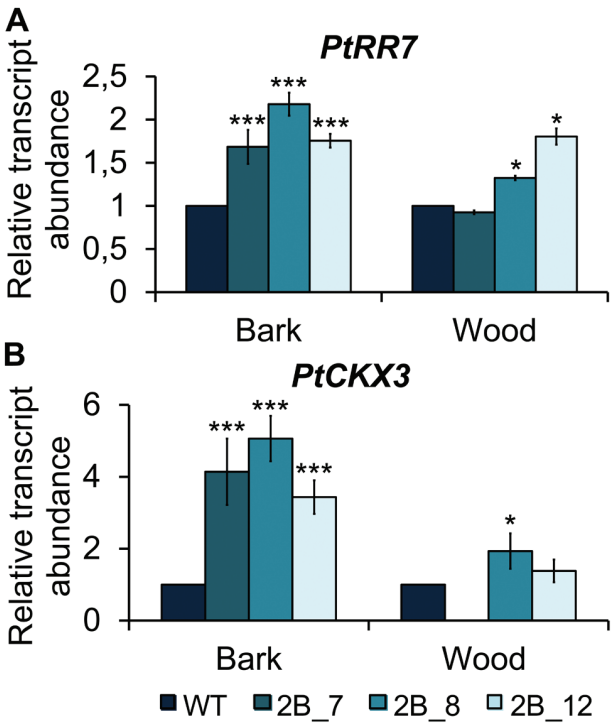

Fig. 6. Expression of genes involved in cytokinin function, determined at the stem base (ENbase) corresponding to an internode between the 20th and 25th internodes, in the *35S:PtSHR2B* hybrid aspen plants grown in a greenhouse for 10 weeks. (A, B) Relative transcript levels of (A) the cytokinin primary response gene, *PtRR7*, and (B) the cytokinin oxidase gene, *PtCKX3*, in bark and wood tissues of *35S:PtSHR2B* trees. Values are the means ±SE of at least three biological replicates and two technical replicates, and asterisks indicate the significance of the difference between each individual line and the wild type (**P*<0.05, ***P*<0.01, and ****P*<0.001, Mann–Whitney U-test). (This figure is available in colour at *JXB* online.)

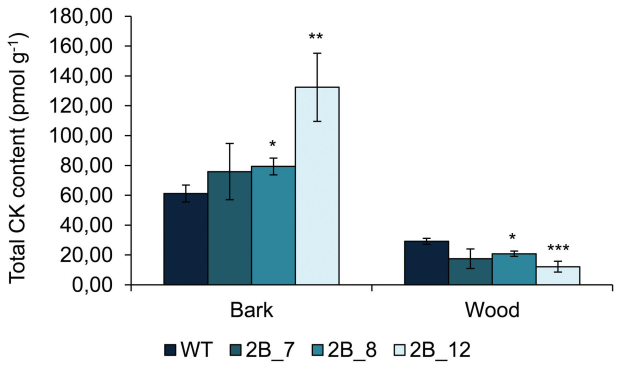

Fig. 7. Cytokinin (CK) content in the bark and wood tissues of *35S:PtSHR2B* hybrid aspen plants grown in a greenhouse for 10 weeks. Values are the means ±SE of at least three biological replicates, and asterisks indicate the significance between each individual line and the wild type (**P*<0.05, ***P*<0.01, and ****P*<0.001, one-way ANOVA). (This figure is available in colour at *JXB* online.)

PtSHR2B promoter drove *GUS* expression in the phellogen. *PtSHR1* has previously been reported to be expressed in the vascular cambium, and to regulate its activity (Schrader *et al.*, 2004; Wang *et al.*, 2011). Furthermore, AtSHR and PtSHR1 have been shown to have broad activity in meristems in the roots and shoots (Schrader *et al.*, 2004; Wang *et al.*, 2011). However, this is the first work reporting an *SHR*-like gene promoter activity in the phellogen, suggesting that *PtSHR2B* fulfils an important function in this lateral meristem.

This finding led us to explore further the function of *PtSHR2B* by ectopically expressing it in hybrid aspen. Compared with the wild type, overall growth was reduced in transgenic trees as evaluated by several parameters to assess

Table 1. *Distribution of the cytokinin derivatives between bark and wood tissues, in 10 mg of tissue, of 35S:PtSHR2B hybrid aspen plants grown in the greenhouse for 10 weeks*

	CKs	Total	iP types	tZ types	DHZ types	cZ types
Bark	**WT**	61.2±5.8	13.8±1.3	7.8±1.4	2.7±0.4	36.9±3.9
	2B_7	75.9±18.8	6.9±0.1*	10.1±1.8	5.9±0.4*	52.9±16.5*
	2B_8	79.3±5.6*	9.7±0.3	11.0±0.4*	6.7±0.7***	51.9±5.1*
	2B_12	132±22.8**	5.9±1.4**	14.2±6.6*	6.7±2.9*	86.3±14.6***
Wood	**WT**	29.2±2.0	12.5±0.7	2.7±0.6	0.5±0.1	13.5±1.0
	2B_7	17.5±6.5	4.4±1.9**	2.3±1.0	0.8±0.3	9.9±3.8
	2B_8	20.8±1.8*	5.2±0.8**	2.6±0.3	0.7±0.008**	12.4±0.7
	2B_12	12.2±3.7***	4.3±1.8***	1.8±0.6	0.7±0.3	5.7±1.2***

Values are means ±SE of at least three biological replicates, and asterisks indicate the significance between each individual line and the wild-type (*P<0.05, **P<0.01, and ***P<0.001, one-way ANOVA).
CK, cytokinin; iP, isopentenyladenine; tZ, *trans*-zeatin; DHZ, dihydrozeatin; cZ, *cis*-zeatin.

primary and secondary growth. Total tree height and mean internode length between EN10 and EN17 were amongst the most significantly reduced growth parameters in all the transformed lines. The total number of internodes was only slightly reduced, further indicating that stem elongation was inhibited in the transgenic lines. The stems of the transgenic trees were less tapered than those of the wild-type plants since both groups had similar stem diameters in the upper region of the stem (at EN14), but the stems of the transgenics were appreciably narrower at the base (EN20–EN25). When the stem tissues were analysed in more detail, we verified a relative reduction in the wood layer, while an increase in the proportion of bark, composed of phloem, phelloderm, and phellem, was observed. We could not correlate the increase in the bark width with an increase of the phellem given that the shedding of cork layer cells in *Populus* occurs simultaneously with cell division of phellogen initials (Kaufert, 1937).

Altogether, the phenotypic analysis of these plants suggests that, in addition to the effect on secondary growth patterns, *PtSHR2B* ectopic expression affects overall plant growth. When studying the function of *PtSHR1* in hybrid aspen, Wang *et al.* (2011) have shown that its partial suppression enhanced overall plant growth, and suggested that the protein acts as a dose-dependent negative regulator of meristem activity. Our results do not allow a conclusion to be drawn on the dose-dependent action of PtSHR2B but support that it might interfere in plant growth through similar mechanisms to those of *PtSHR1*.

In order to investigate the possible mechanisms by which *PtSHR2B* may exert its function, we have analysed the expression of the CK-related genes *PtRR7* and *PtCKX3,* which encode a CK primary response and a CK degradation protein, respectively. As inducers of cell division and differentiation, CKs are central regulators of plant development (Miyawaki *et al.*, 2006; Sakakibara, 2006). In fact, the importance of CK signalling in the regulation of cambial activity in *Populus* stems has been previously demonstrated (Nieminen *et al.*, 2008). In our work, we found that the expression of both genes was significantly up-regulated in the bark tissues of all the transgenic lines, but their expression levels were either similar or only slightly increased in the wood tissues when compared with the wild type. *PtRR7* transcript levels were reported to be positively correlated with the amount of CK present across the stems of hybrid aspen trees (Nieminen *et al.*, 2008). Cytokinin oxidase gene expression has also been shown to be up-regulated in response to increased CK levels (Motyka *et al.*, 1996; Jiao *et al.*, 2003). Additionally, in *Arabidopsis*, the *CKX3* transcript levels were significantly reduced in the *shr* roots (Cui *et al.*, 2011). Our transcript quantification results would seem consistent with increased CK endogenous levels in the tissues where expression is higher. In fact, through quantification of CKs we were able to confirm that endogenous total CK levels were significantly higher in the bark tissues, in two out of the three transgenic lines. This trend was not verified in wood tissues that, despite the lower CK levels in two out of three lines, showed a slight up-regulation of *PtRR7*. Differences in CK biosynthesis and homeostasis regulation, or even their crosstalk with auxin in the vascular tissues may contribute to explain this observation (Kieber and Schaller, 2014), although additional studies would be required to clarify this issue.

The mechanisms by which the overexpression of *PtSHR2B* might lead to increased CK levels in the bark tissues were not addressed in our study. However, it is tempting to speculate that similarly to *AtSHR* (Sebastian *et al.*, 2015), *PtSHR2B* may interfere with CK homeostasis. It is possible that the increased CK levels in the bark (containing the phellogen layer) result from an increased amount of *PtSHR2B* transcripts which may regulate target genes with specific domains of expression in these tissues. The decrease in the wood layer, indicative of modified cambium activity, might also be explained by the slightly reduced levels of total CKs in the wood tissues. This will need to be tested in future studies with tissue-specific promoters, since secondary effects of ectopic expression of *PtSHR2B* cannot be ruled out.

The data presented here suggest that *PtSHR2B* is involved in lateral meristem functioning. Although it cannot be excluded that *PtSHR2B* plays a role alongside *PtSHR1* in regulating vascular cambium activity, our data suggest that speciation and functional diversification have led to these two *AtSHR* homologues playing different roles in *Populus* stems. *PtSHR2B* appears to function principally in the phellogen

and therefore in the regulation of phellem and periderm formation. This finding may contribute to strategies aimed at the selection and improvement of species such as cork oak in which, unlike *Populus*, the phellogen is active throughout the entire tree lifespan, being at the basis of a highly profitable cork industry.

Supplementary data

Supplementary data are available at *JXB* online.

Figure S1. Schematic representation of tissue sampling, stem section measurements, and anatomical aspects of hybrid aspen stem.

Figure S2. Growth curves of the wild-type and *35S:PtSHR2B* hybrid aspen plants.

Acknowledgments

We thank Dr Paula Scotti Campos (Instituto Nacional de Investigação Agrária e Veterinária, I. P., Oeiras, Portugal) for making available the equipment of the leaf area meter. The authors also sincerely thank Eva Hirnerová for her help with phytohormone analyses. This work was supported by Fundação para a Ciência e Tecnologia, through Research unit GREEN-it 'Bioresources for Sustainability' (UID/Multi/04551/2013 and projects PEst-OE/EQB/LA0004/2011, PTDC/AGR-GPL/098369/2008, and IF/01168/2013), and grants SFRH/BD/44474/2008 (to Andreia Miguel) and SFRH/BD/30074/2006 (to Ana Milhinhos). ON was funded by the Ministry of Education, Youth and Sports of the Czech Republic (the National Program for Sustainability I Nr. LO1204, and the 'Návrat' program LK21306).

References

Abràmoff MD, Magalhães PJ, Ram SJ. 2004. Image processing with ImageJ. Biophotonics International **11,** 36–42.

Antoniadi I, Plačková L, Simonovik B, Doležal K, Turnbull C, Ljung K, Novák O. 2015. Cell-type-specific cytokinin distribution within the Arabidopsis primary root apex. The Plant Cell **27,** 1955–1967.

Baucher M, El Jaziri M, Vandeputte O. 2007. From primary to secondary growth: origin and development of the vascular system. Journal of Experimental Botany **58,** 3485–3501.

Benfey PN, Linstead PJ, Roberts K, Schiefelbein JW, Hauser MT, Aeschbacher RA. 1993. Root development in *Arabidopsis*: four mutants with dramatically altered root morphogenesis. Development **119,** 57–70.

Blanc G, Wolfe KH. 2004. Functional divergence of duplicated genes formed by polyploidy during Arabidopsis evolution. The Plant Cell **16,** 1679–1691.

Bolle C. 2004. The role of GRAS proteins in plant signal transduction and development. Planta **218,** 683–692.

Brand U, Fletcher J, Hobe M, Meyerowitz E, Simon R. 2000. Dependence of stem cell fate in *Arabidopsis* on a feedback loop regulated by *CLV3* activity. Science **289,** 617–619.

Brunner AM, Yakovlev IA, Strauss SH. 2004. Validating internal controls for quantitative plant gene expression studies. BMC Plant Biology **4,** 14.

Carlsbecker A, Lee J-Y, Roberts CJ, *et al*. 2010. Cell signalling by microRNA165/6 directs gene dose-dependent root cell fate. Nature **465,** 316–321.

Carretero-Paulet L, Fares MA. 2012. Evolutionary dynamics and functional specialization of plant paralogs formed by whole and small-scale genome duplications. Molecular Biology and Evolution **29,** 3541–3451.

Chang S, Puryear J, Cairney J. 1993. A simple and efficient method for isolating RNA from pine trees. Plant Molecular Biology Reporter **11,** 113–116.

Cui H, Hao Y, Kovtun M, Stolc V, Deng X-W, Sakakibara H, Kojima M. 2011. Genome-wide direct target analysis reveals a role for SHORT-ROOT in root vascular patterning through cytokinin homeostasis. Plant Physiology **157,** 1221–1231.

Dhondt S, Coppens F, De Winter F, Swarup K, Merks RMH, Inzé D, Bennett MJ, Beemster GTS. 2010. SHORT-ROOT and SCARECROW regulate leaf growth in Arabidopsis by stimulating S-phase progression of the cell cycle. Plant Physiology **154,** 1183–1195.

Di Laurenzio L, Wysocka-diller J, Malamy JE, Pysh L, Helariutta Y, Freshour G, Hahn MG, Feldmann KA, Benfey PN. 1996. The *SCARECROW* gene regulates an asymmetric cell division that is essential for generating the radial organization of the Arabidopsis root. Cell **86,** 423–433.

Du J, Groover A. 2010. Transcriptional regulation of secondary growth and wood formation. Journal of Integrative Plant Biology **52,** 17–27.

Du J, Mansfield SD, Groover AT. 2009. The *Populus* homeobox gene *ARBORKNOX2* regulates cell differentiation during secondary growth. The Plant Journal **60,** 1000–1014.

Du J, Miura E, Robischon M, Martinez C, Groover A. 2011. The *Populus* Class III HD ZIP transcription factor *POPCORONA* affects cell differentiation during secondary growth of woody stems. PLoS One **6,** e17458.

Emery JF, Floyd SK, Alvarez J, Eshed Y, Hawker NP, Izhaki A, Baum SF, Bowman JL. 2003. Radial patterning of *Arabidopsis* shoots by Class III HD-ZIP and KANADI genes. Current Biology **13,** 1768–1774.

Evert RF. 2006. Periderm. In: Esau`s plant anatomy meristems, cells and tissues of the plant body—their structure, function, and development . Chichester: John Wiley and Sons , 427–445.

Fukaki H, Wysocka-Diller J, Kato T, Fujisawa H, Benfey PN, Tasaka M. 1998. Genetic evidence that the endodermis is essential for shoot gravitropism in *Arabidopsis thaliana*. The Plant Journal **14,** 425–430.

Groover AT, Mansfield SD, DiFazio SP, Dupper G, Fontana JR, Millar R, Wang Y. 2006. The *Populus* homeobox gene *ARBORKNOX1* reveals overlapping mechanisms regulating the shoot apical meristem and the vascular cambium. Plant Molecular Biology **61,** 917–932.

Ha S, Vankova R, Yamaguchi-Shinozaki K, Shinozaki K, Tran LSP. 2012. Cytokinins: metabolism and function in plant adaptation to environmental stresses. Trends in Plant Science **17,** 172–179.

Haecker A, Gross-Hardt R, Geiges B, Sarkar A, Breuninger H, Herrmann M, Laux T. 2004. Expression dynamics of *WOX* genes mark cell fate decisions during early embryonic patterning in *Arabidopsis thaliana*. Development **131,** 657–668.

Hao Y, Cui H. 2012. SHORT-ROOT regulates vascular patterning, but not apical meristematic activity in the Arabidopsis root through cytokinin homeostasis. Plant Signaling and Behavior **7,** 314–317.

Helariutta Y, Fukaki H, Wysocka-Diller J, Nakajima K, Jung J, Sena G, Hauser MT, Benfey PN. 2000. The *SHORT-ROOT* gene controls radial patterning of the Arabidopsis root through radial signaling. Cell **101,** 555–567.

Hellemans J, Mortier G, De Paepe A, Speleman F, Vandesompele J. 2007. qBase relative quantification framework and software for management and automated analysis of real-time quantitative PCR data. Genome Biology **8,** R19.

Jiao S, Hantke S, Zinselmeier C, *et al*. 2003. Cytokinin oxidase gene expression in maize is localized to the vasculature, and is induced by cytokinins, abscisic acid, and abiotic stress. Plant Physiology **132,** 1228–1240.

Karimi M, Inzé D, Depicker A. 2002. Gateway vectors for Agrobacterium-mediated plant transformation. Trends in Plant Science **7,** 193–195.

Kaufert F. 1937. Factors influencing the formation of periderm in aspen. American Journal of Botany **24,** 24–30.

Kieber JJ, Schaller GE. 2014. Cytokinins. The Arabidopsis Book **12,** e0168.

Koizumi K, Hayashi T, Wu S, Gallagher KL. 2012. The SHORT-ROOT protein acts as a mobile, dose-dependent signal in patterning the ground tissue. Proceedings of the National Academy of Sciences, USA **109,** 13010–13015.

Levesque MP, Vernoux T, Busch W, *et al*. 2006. Whole-genome analysis of the SHORT-ROOT developmental pathway in *Arabidopsis*. PLoS Biology **4,** e143.

Liebsch D, Sunaryo W, Holmlund M, *et al*. 2014. Class I KNOX transcription factors promote differentiation of cambial derivatives into xylem fibers in the *Arabidopsis* hypocotyl. Development **141,** 4311–4319.

Livak KJ, Schmittgen TD. 2001. Analysis of relative gene expression data using real-time quantitative PCR and the 2^(-Delta Delta CT) Method. Methods **25,** 402–408.

Long JA, Moan EI, Medford JI, Barton MK. 1996. A member of the KNOTTED class of homeodomain proteins encoded by the *STM* gene of *Arabidopsis*. Nature **379,** 66–69.

Marum L, Miguel A, Ricardo CP, Miguel C. 2012. Reference gene selection for quantitative real-time PCR normalization in *Quercus suber*. PLoS One **7,** 1–10.

Mayer KF, Schoof H, Haecker A, Lenhard M, Jürgens G, Laux T. 1998. Role of *WUSCHEL* in regulating stem cell fate in the *Arabidopsis* shoot meristem. Cell **95,** 805–815.

Mele G, Ori N, Sato Y, Hake S. 2003. The *knotted1*-like homeobox gene *BREVIPEDICELLUS* regulates cell differentiation by modulating metabolic pathways. Genes and Development **17,** 2088–2093.

Milhinhos A, Prestele J, Bollhöner B, *et al*. 2013. Thermospermine levels are controlled by an auxin-dependent feedback loop mechanism in *Populus* xylem. The Plant Journal **75,** 685–698.

Miyawaki K, Tarkowski P, Matsumoto-Kitano M, Kato T, Sato S, Tarkowska D, Tabata S, Sandberg G, Kakimoto T. 2006. Roles of *Arabidopsis* ATP/ADP isopentenyltransferases and tRNA isopentenyltransferases in cytokinin biosynthesis. Proceedings of the National Academy of Sciences, USA **103,** 16598–16603.

Motyka V, Faiss M, Strnad M, Kamínek M, Schmülling T. 1996. Changes in cytokinin content and cytokinin oxidase activity in response to derepression of ipt gene transcription in transgenic tobacco calli and plants. Plant Physiology **112,** 1035–1043.

Murashige T, Skoog F. 1962. A revised medium for rapid growth and bio assays with tobacco tissue cultures. Physiologia Plantarum **15,** 473–497.

Nakajima K, Sena G, Nawy T, Benfey PN. 2001. Intercellular movement of the putative transcription factor SHR in root patterning. Nature **413,** 307–311.

Nieminen K, Immanen J, Laxell M, *et al*. 2008. Cytokinin signaling regulates cambial development in poplar. Proceedings of the National Academy of Sciences, USA **105,** 20032–20037.

Nilsson O, Aldén T, Sitbon F, Anthony Little CH, Chalupa V, Sandberg G, Olsson O. 1992. Spatial pattern of cauliflower mosaic virus 35S promoter-luciferase expression in transgenic hybrid aspen trees monitored by enzymatic assay and non-destructive imaging. Transgenic Research **1,** 209–220.

Paquette AJ, Benfey PN. 2005. Maturation of the ground tissue of the root is regulated by gibberellin and *SCARECROW* and requires *SHORT-ROOT*. Plant Physiology **138,** 636–640.

Pfaffl MW. 2001. A new mathematical model for relative quantification in real-time RT–PCR. Nucleic Acids Research **29,** e45.

Ramírez-Carvajal GA, Morse AM, Davis JM. 2008. Transcript profiles of the cytokinin response regulator gene family in Populus imply diverse roles in plant development. New Phytologist **177,** 77–89.

Reid KE, Olsson N, Schlosser J, Peng F, Lund ST. 2006. An optimized grapevine RNA isolation procedure and statistical determination of reference genes for real-time RT–PCR during berry development. BMC Plant Biology **6,** 27.

Robischon M, Du J, Miura E, Groover A. 2011. The *Populus* class III HD ZIP, *popREVOLUTA*, influences cambium initiation and patterning of woody stems. Plant Physiology **155,** 1214–1225.

Rodgers-Melnick E, Mane SP, Dharmawardhana P, Slavov GT, Crasta OR, Strauss SH, Brunner AM, Difazio SP. 2012. Contrasting patterns of evolution following whole genome versus tandem duplication events in *Populus*. Genome Research **22,** 95–105.

Sakakibara H. 2006. Cytokinins: activity, biosynthesis, and translocation. Annual Review of Plant Biology **57,** 431–449.

Sanchez P, Nehlin L, Greb T. 2012. From thin to thick: major transitions during stem development. Trends in Plant Science **17,** 113–121.

Sarkar AK, Luijten M, Miyashima S, Lenhard M, Hashimoto T, Nakajima K, Scheres B, Heidstra R, Laux T. 2007. Conserved factors regulate signalling in *Arabidopsis thaliana* shoot and root stem cell organizers. Nature **446,** 811–814.

Schneider CA, Rasband WS, Eliceiri KW. 2012. NIH Image to ImageJ: 25 years of image analysis. Nature Methods **9,** 671–675.

Schoof H, Lenhard M, Haecker A, Mayer KF, Jürgens G, Laux T. 2000. The stem cell population of *Arabidopsis* shoot meristems in maintained by a regulatory loop between the *CLAVATA* and *WUSCHEL* genes. Cell **100,** 635–644.

Schrader J, Nilsson J, Mellerowicz E, Berglund A, Nilsson P, Hertzberg M. 2004. A high-resolution transcript profile across the wood-forming meristem of poplar identifies potential regulators of cambial stem cell identity. The Plant Cell **16,** 2278–2292.

Schuetz M, Smith R, Ellis B. 2012. Xylem tissue specification, patterning, and differentiation mechanisms. Journal of Experimental Botany **64,** 11–31.

Sebastian J, Ryu KH, Zhou J, Tarkowská D, Tarkowski P, Cho Y-H, Yoo S-D, Kim E-S, Lee J-Y. 2015. PHABULOSA controls the quiescent center-independent root meristem activities in *Arabidopsis thaliana*. PLoS Genetics **11,** e1004973.

Seoighe C, Gehring C. 2004. Genome duplication led to highly selective expansion of the Arabidopsis thaliana proteome. Trends in Genetics **20,** 461–464.

Silva SP, Sabino MA, Fernandes EM, Correlo VM, Boesel LF, Reis RL. 2005. Cork: properties, capabilities and applications. International Materials Reviews **50,** 345–365.

Solé A, Sánchez C, Vielba JM, Valladares S, Abarca D, Díaz-Sala C. 2008. Characterization and expression of a *Pinus radiata* putative ortholog to the *Arabidopsis SHORT-ROOT* gene. Tree Physiology **28,** 1629–1639.

Soler M. 2008. Molecular genetics of cork formation. PhD Thesis, Girona University.

Sozzani R, Cui H, Moreno-Risueno MA, Bush W, Van Norman JM, Vernoux T, Brady SM, Dewitte W, Murray JAH, Benfey PN. 2010. Spatiotemporal regulation of cell-cycle genes by SHORTROOT links patterning and growth. Nature **466,** 128–132.

Stahl Y, **Simon R.** 2009. Is the Arabidopsis root niche protected by sequestration of the CLE40 signal by its putative receptor ACR4? Plant Signaling and Behavior **4,** 634–635.

Stahl Y, Wink RH, Ingram GC, Simon R. 2009. A signaling module controlling the stem cell niche in *Arabidopsis* root meristems. Current Biology **19,** 909–914.

Svačinová J, Novák O, Plačková L, Lenobel R, Holík J, Strnad M, Doležal K. 2012. A new approach for cytokinin isolation from Arabidopsis tissues using miniaturized purification: pipette tip solid-phase extraction. Plant Methods **8,** 17.

Tucker MR, Laux T. 2007. Connecting the paths in plant stem cell regulation. Trends in Cell Biology **17,** 403–410.

Tuskan GA, DiFazio S, Jansson S, Bohlmann J, Grigoriev I, Hellsten U, Putnam N. 2006. The genome of black cottonwood, *Populus trichocarpa* (Torr. & Gray). Science **313,** 1596–1604.

Wang J, Andersson-Gunnerås S, Gaboreanu I, *et al*. 2011. Reduced expression of the SHORT-ROOT gene increases the rates of growth and development in hybrid poplar and Arabidopsis. PLoS One **6,** e28878.

Zhao S, Fernald RD. 2005. Comprehensive algorithm for quantitative real-time polymerase chain reaction. Journal of Computational Biology **12,** 1047–64.